

Optimizing Deep CNN-Based Queries over Video Streams at Scale

Daniel Kang, John Emmons, Firas Abuzaid, Peter Bailis, Matei Zaharia
Stanford InfoLab

ABSTRACT

Video is one of the fastest-growing sources of data and is rich with interesting semantic information. Furthermore, recent advances in computer vision, in the form of deep convolutional neural networks (CNNs), have made it possible to query this semantic information with near-human accuracy (in the form of image tagging). However, performing inference with state-of-the-art CNNs is computationally expensive: analyzing videos in real time (at 30 frames/sec) requires a \$1200 GPU per video stream, posing a serious computational barrier to CNN adoption in large-scale video data management systems. In response, we present NOSCOPe, a system that uses cost-based optimization to assemble a specialized video processing pipeline for each input video stream, greatly accelerating subsequent CNN-based queries on the video. As NOSCOPe observes a video, it trains two types of pipeline components (which we call filters) to exploit the locality in the video stream: *difference detectors* that exploit temporal locality between frames, and *specialized models* that are tailored to a specific scene and query (i.e., exploit environmental and query-specific locality). We show that the optimal set of filters and their parameters depends significantly on the video stream and query in question, so NOSCOPe introduces an efficient cost-based optimizer for this problem to select them. With this approach, our NOSCOPe prototype achieves up to 120-3,200 \times speed-ups (318-8,500 \times real-time) on binary classification tasks over real-world webcam and surveillance video while maintaining accuracy within 1-5% of a state-of-the-art CNN.

1. INTRODUCTION

Video represents an immense proportion of data collected and managed at scale today. Three hundred hours of video are uploaded to YouTube every minute [3], and 70% of all Internet traffic in 2015 was due to video data [2]. Given the increasing consumer and industrial appetites for *real-time* video content—from social media platforms including Facebook Live, Periscope, and Twitch to large-scale industrial monitoring systems—and the decreased cost of video capture (via inexpensive sensors, wearables, and the Internet of Things), the rate of video data collection will only accelerate.

How can we query these lifetimes of video? For example, given

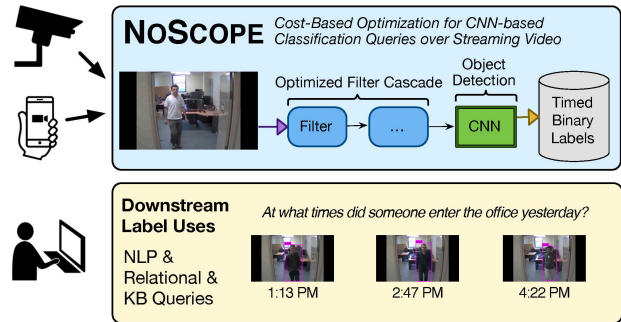


Figure 1: High-level overview and potential downstream uses of the outputs of the NOSCOPe system. NOSCOPe applies state-of-the-art CNNs to video streams, performing binary classification over video contents. To maintain accuracy while dramatically improving runtime, NOSCOPe performs query optimization of a cascade of specialized operators based on video contents.

the video streams from a university campus, we might ask: how long is the line at each café right now, or how many people use the north parking lot each day? At scale, it is infeasible to answer these questions manually; instead, machines must extract this semantic information from video. The literature offers a wealth of existing proposals for storing [6, 47], querying [5, 30, 45, 58, 80], and managing [32, 42, 75] video data, largely based on conventional computer vision techniques. However, new techniques in computer vision have greatly improved accuracy. A combination of inexpensive parallel hardware (GPUs), quality training data (e.g., ImageNet [67]), and algorithmic breakthroughs [44] have led to the development of deep *convolutional neural networks* (CNNs) [34, 46] that can accurately perform semantic tagging and labeling of visual content, recognizing thousands of classes of objects [67], and even outperform human experts at tasks such as cancer diagnosis [27, 76].

It is difficult to understate the impact of CNNs on modern computer vision and visual data processing. For example, in 2012, only one team of seven in the ImageNet classification competition (Krizhevsky et al. [44]) used a CNN, and the CNN won out over conventional techniques such as SIFT, HOG, and SVMs. In 2016, all entrants employed CNNs. Moreover, 2012’s winning model would have scored dead last in 2016, making more than five times as many errors as 2016’s best model [67]. CNNs now power major functionality at Facebook, Instagram, Twitter, Google, Apple, and a host of autonomous vehicle companies [53]. Given this revolution in computer vision, we believe it is critical to re-evaluate the integration of data management and computer vision.

Specifically, CNNs offer the ability to extract highly accurate labels from data for a variety of downstream processing tasks (e.g., in spatiotemporal queries [18], integration with relational data and

knowledge bases [77], alerting [35]). However, simply applying CNNs to video data at scale is prohibitively expensive. CNNs’ superb statistical performance comes at a severe computational cost: the computer vision community’s fastest models for accurate object detection run at 30-60 frames per second (i.e., 1-2 \times real time) on a state-of-the-art NVIDIA Titan X GPU (\$1200 at time of writing) [15, 64–66].¹ Given continued decreases in image sensor costs, these computational overheads create a three-plus order-of-magnitude imbalance between cost of video data acquisition and cost of CNN-based processing. For example, processing all new YouTube uploads in real-time would require over \$44M in GPU hardware alone, without even considering the cost of power. Moreover, in a field obsessed with accuracy, CNNs continue to get deeper and more expensive to evaluate; for example, Google’s winning CNN model in the 2014 ImageNet competition had 22 layers, while Microsoft’s winning model in 2015 had 152 layers [38].

In this paper, we address this tension between CNNs’ accuracy and computational expense by employing one of the mainstays of data management system design: query optimization. We develop a system called NOSCOPE that queries the contents of video streams using state-of-the-art CNNs—but up to 120-3,200 \times faster (i.e., 318-8,500 \times real-time) with limited (i.e., 1-5%) loss in accuracy (Section 9). Just as conventional database engines automatically adapt their query processing plans to properties of the data [68], NOSCOPE automatically adapts CNN-based video query processing to the contents of video streams. Given a target object class (e.g., people, buses, dogs), a target video stream, and a reference CNN (e.g., YOLOv2 [64]), NOSCOPE performs binary classification of the data stream to extract occurrences of the target objects. However, instead of simply running the reference CNN on the stream, NOSCOPE configures and executes a sequence (i.e., cascade [73]) of cheaper *filters* that approximate the reference CNN to a specified target accuracy. As we show, the optimal filter configuration is highly dependent on the target video and the target query. Therefore, NOSCOPE automatically optimizes the filter cascade structure and parameters of individual filters (e.g., confidence thresholds) based on estimates of filter execution cost and properties of the video stream (e.g., activity level, scene complexity). As a result, NOSCOPE allows efficient and accurate classification and label extraction of data streams—without requiring manual tuning.

In its search for equivalent but efficient CNN filters, NOSCOPE exploits a key property of video data: video content is often highly redundant. NOSCOPE employs two types of filters that exploit several types of locality (i.e., similarities) within a stream. First, video data exhibits *temporal locality*. Consider the following frames, which appeared sequentially on a public webcam in Taipei:



Unsurprisingly, these frames are nearly identical. To exploit this locality, instead of running the full CNN on each frame, NOSCOPE can train one of several low-cost *difference detectors* (based on histograms of frame content) that indicate whether the contents of video have changed significantly. Second, video exhibits *scene-specific spatial locality*. While CNNs can recognize objects from

¹In this work, we focus specifically on multi-scale object detection (i.e., identifying instances of an object regardless of its scale in the image) [15, 64–66]; these techniques are more expensive than models that take in an image centered on the object, but they are required to find objects in most realistic video applications.

many angles, many video streams have limited viewing angles. Consider the following five buses, also from the Taipei stream:



In this video stream, objects such as the above buses only appear in a small set of perspectives; we need not consider arbitrary rotations and translations of the objects. In addition, as a third form of locality, we can leverage *query-specific locality*; while queries may only seek to identify a small number of classes (e.g., buses), CNNs are pre-trained to recognize thousands of objects, from sheep to apples to tennis rackets. To capitalize on this scene-specific and query-specific locality, NOSCOPE can train *specialized models*—smaller CNNs that are tailored to a given video stream and to a fixed class of labels. NOSCOPE then executes these specialized models, consulting the full CNN only when the smaller models are uncertain (i.e., produce results with confidence below an automatically learned threshold).

The key challenge in exploiting the above observations is that the optimal configuration of filters is highly data-dependent. Diverse filters will perform very differently on different scenes, offering distinct tradeoffs between speed, selectivity, and accuracy. For example, a difference detector based on subtraction from the previous frame might work well on mostly static scenes but may only add overhead in a video overseeing a busy highway. Likewise, the complexity of specialized CNN models required to effectively recognize different object classes varies widely based on both the object class and the scene. Even setting the detection thresholds of the filters is a trade-off: should we make a difference detector’s threshold less aggressive to reduce its false negative rate, or should we make it more aggressive to eliminate more frames early in the pipeline and avoid calling an expensive CNN?

To solve this problem, NOSCOPE introduces a cost-based optimizer that can efficiently select the fastest combination of filters for a video stream and query given an accuracy target. The optimizer empirically applies each filter to a sample of the data once, and then computes the optimal thresholds for each combination of filters using an efficient linear parameter sweep through the space of feasible thresholds. It can be executed in time comparable to labeling the sample data using an expensive CNN (an unavoidable step in obtaining such data) to automatically select a filter cascade.

We evaluate a NOSCOPE prototype on fixed-angle binary classification tasks including pedestrian detection and automotive detection as found in monitoring and surveillance applications. NOSCOPE achieves speedups of up to 3,200 \times over general-purpose state-of-the-art CNNs while retaining high accuracy (95-99%) across a range of streams. To summarize, our contributions are:

1. NOSCOPE, the first data management system that accelerates CNN-based classification queries over video streams at scale.
2. CNN-specific techniques for difference detection across frames and model specialization for a given stream and query, as well as a cost-based optimizer that can automatically identify the best combination of these filters for a given accuracy target.
3. An evaluation of NOSCOPE on fixed-angle binary classification showing up to 3,200 \times speedups on real-world data.

2. BACKGROUND

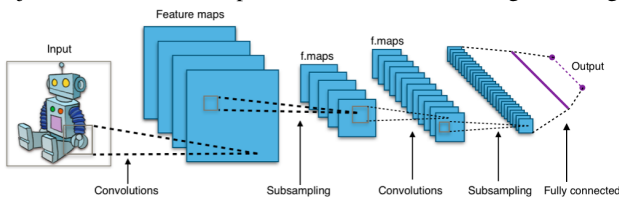
Extracting semantic information and labels from visual data is a core focus of computer vision. Given an input image, a host of computer vision methods can extract information including object

types and their location. Thus, from a data management perspective, computer vision can act as a valuable information extraction tool. In this section, we provide background on these methods, focusing on object detection tasks: given an image, what objects does it contain?

Classic Methods and Databases. Methods for automated object detection date to at least the 1960s [60], and classic techniques [51, 71, 79] combine machine learning methods such as classification and clustering with image-specific featurization techniques such as SIFT [50]. Data management researchers have long recognized the potential of these classic techniques for organizing and querying visual data—starting with early systems such as Chabot [57] and QBIC [30], and followed by a range of “multimedia” databases for storing [6, 47], querying [5, 45, 58, 80], and managing [32, 42, 75] video data. Similar techniques were deployed in commercial software such as Oracle Multimedia and Google Image Search. Nonetheless, most of these systems only use simple, *low-level* image features (e.g., colors, textures and segments), and many of them rely on augmenting video with text for richer semantic queries.

The (C)NN Revolution. Following these early successes, the past five years have seen a sea change in the research and practice of computer vision. Specifically, artificial neural networks—which date to the 1940s—have dramatically improved accuracy to near-human or better-than-human levels. With immense amounts of hand-labeled training data (e.g., the ImageNet benchmark developed in 2010), availability of commodity parallel hardware (GPUs), and advances in model training (e.g., dropout), training “deep” models with millions to billions of parameters has not only become feasible but now is the preferred method for accurate computer vision tasks spanning image classification [67], pedestrian detection [78], and automatic captioning [26]. These networks power image processing tasks at online services including Google, Facebook, Instagram, and Amazon as well as real-world tasks including autonomous driving. In this section, we provide a brief overview of CNN training and evaluation for the task of object detection in video, with binary output: for example, when does the video include a person?

CNN Basics. A *convolutional neural network* [34] consists of a series of connected *layers* that can process a high-dimensional input image and output a simpler representation. Each layer of the CNN corresponds to a step in computation, and each CNN contains a combination of *convolutional* layers (that apply convolution operators over tiles to “combine” nearby pixels), *pooling* layers (that reduce the dimensionality of the subsequent layers), *rectified linear units (ReLU)* layers (that perform non-linear transformation on each input), and a *fully connected* layer (that outputs the actual prediction based on the prior layer). As illustrated below [1], combining multiple such layers in a “deep” architecture and by fitting the appropriate weights of the computation (i.e., the “neurons”) between stages, CNNs can learn the structure of common objects and detect their presence and absence in a given image.



Depending on the task, the best model architecture (e.g., configuration of layers) varies, but the overwhelming trend has been to build deeper models given more training data.

CNN Training. Training CNNs consists of fitting appropriate neuron weights to a given architecture such that the overall empirical

error on a given set of labeled training data is minimized. This process is very computationally expensive, but is now supported by a wide range of software frameworks such as Google TensorFlow, Torch and Caffe. To train an object detector on video, we would first label a portion of a video (or set of videos) by hand, marking which frames contained people and which did not. Subsequently, we would feed each frame to a CNN training framework. Conceptually, compared to prior computer vision approaches that relied heavily on manually designed features (e.g., gradients and edges [50, 71]), CNNs automatically learn both low-level and high-level features from the training dataset. Due to the computational cost of training CNNs, companies and researchers have also published hundreds of pre-trained models, each representing thousands of hours of CPU and GPU training time. These off-the-shelf, high-quality models are easy to apply on new data, as we do (faster) in NOSCOPE.

CNN Evaluation. Evaluating CNNs on video consists—almost exclusively and perhaps surprisingly—of passing frames to a CNN one frame at a time. That is, to detect objects in a video, we evaluate a CNN repeatedly, once per frame. This is for several reasons. First, CNNs are almost always trained on large, static *images*, not on moving video. Therefore, evaluating them on video by converting them to a series of static images is easy (if expensive). Second, historically, the resurgence of interest in CNNs has been driven by competitions such as ImageNet, in which the only metric of interest is *accuracy*, not evaluation (i.e., inference) speed. In 2016, the difference between the first- and second-place models in ImageNet’s object recognition competition was 0.72% (2.991% vs. 3.711% top-5 classification error; in contrast, humans achieve approximately 5.1% error). Therefore, with few exceptions [31], even if highly accurate accelerated methods exist in the design space, they are not favored by the most prestigious competitions in the field. Finally, the handful of object recognition CNNs that are optimized for inference time primarily use “real time” (i.e., 30 frames per second) as their baseline [15, 64, 65], aiming to evaluate one video stream in real time on a GPU. In contrast, we are interested in scaling to thousands of hours of video, possibly from thousands of data streams, for the purposes of large-scale video ingestion and extraction; real time performance is not nearly fast enough for our target applications.

3. NOSCOPE ARCHITECTURE

In this section, we introduce the NOSCOPE system architecture, which automatically selects and trains a set of filters to label the majority of video frames at speeds significantly faster than real-time.

Query Interface. NOSCOPE currently supports binary classification queries based on the labels outputted by the target CNN. For example, a CNN such as YOLO9000 [64] can recognize 9000 classes of objects, including humans, cars, trees, airplanes, etc. Users select one of these classes as a query, and NOSCOPE outputs the time intervals in each stream when an object of that class was visible. Thus, as input, NOSCOPE takes a *target model* (a full-scale CNN trained to recognize objects in images), a subset of labels produced by the target model (specifying an object class to find in the data), and a set of video streams to operate on. Given these inputs, the system’s goal is to *produce the same query result as applying the target model on all frames of the video, at a substantially lower computational cost*. Specifically, NOSCOPE’s optimizer takes at input target false positive and false negative rates and aims to maximize throughput subject to staying within these rates.²

² A false positive is a case where NOSCOPE reports an object but running the original target CNN would have reported no object. A false negative is a case where NOSCOPE reports no object but the target CNN would have reported one.

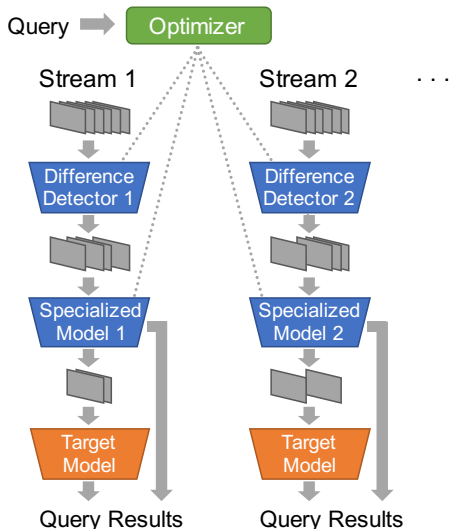


Figure 2: NOSCOPE design. NOSCOPE’s optimizer selects a *different* configuration of difference detectors and specialized models for each video stream to perform binary classification as quickly as possible without calling the full target CNN.

System Components. NOSCOPE includes three key components, as shown in Figure 2. When first provided a new video stream, NOSCOPE applies the target model to all of its frames in order to begin answering the query. However, as it runs, NOSCOPE trains a cascade of *filter* operators to accelerate the specific query on this specific stream.³

NOSCOPE inserts two types of filter operators. First, NOSCOPE uses *difference detectors* (Section 4) to check whether the current frame is similar to another recent frame, or more generally to a reference image whose label is known (e.g., for a camera looking at a hallway, this could be an image where the hallway is empty). Second, NOSCOPE can train *specialized models* (Section 5) that answer the query without passing the frame to the full CNN on “easy” cases. For example, detecting humans with perfect accuracy in all frames may require running the full target CNN, but we show that a much smaller CNN can output a confidence value c that lets us safely label a frame as “no human” if it is below some threshold c_{low} , label it as “human” if $c > c_{\text{high}}$, and pass the frame to the full CNN in between these values.

Finally, to automatically select and configure these filters, NOSCOPE includes a *cost-based optimizer* that learns an efficient configuration of filters to use for each video stream to achieve the target accuracy level (i.e., false positive and false negative rates). As discussed in Section 1, we have found (and later empirically demonstrate) that configuring these filters specifically for each video stream is crucial for performance.

In the next sections, we discuss each of these components in detail. We begin with difference detectors and specialized models in Sections 4 and 5. We then present our optimizer in Section 6. Finally, Section 7 describes our operator implementation and Section 8 discusses the system’s limitations.

4. DIFFERENCE DETECTORS

The first type of filter that NOSCOPE considers attempts to detect differences between images. Figure 3 captures the intuition: the

³ Note that our “filters” are not simply selection operators as in a relational database; they can also make decisions such as labeling the frame early to bypass the downstream target CNN.



(a) empty frame (b) frame with a car (c) subtracted frames
Figure 3: Example of difference detection. The subtracted frame highlights the car that entered the scene.

subtracted frame highlights the car and difference detectors quantify this intuition. Difference detectors are used to determine whether the considered frame is significantly different from another image with known labels. There are two forms of difference detectors supported:

1. Difference detection against a fixed *reference image* for the video stream that is known to contain no objects (from previously calling the target model and seeing no results). For example, for a video of a sidewalk, this might be a frame where the sidewalk is empty. Our implementation computes the reference image by averaging all frames where the target model returns no labels.
2. Difference detection against an *earlier frame*, some configured time t_{diff} seconds into the past. In this case, if there are no significant differences, NOSCOPE returns the same labels that it outputted on the previous frame. Our optimizer learns t_{diff} based on the input data.

We note that the optimal choice between these methods depends on the video, which is why our optimizer selects it automatically. For example, a video of a mostly empty sidewalk might have a natural empty reference image that one can cheaply and confidently compare with to skip many empty frames. In contrast, a video of a city park might always contain some form of mobile objects (e.g., people lying down in the grass), but the objects might move slowly enough that comparing with frames 1 second ago can still eliminate many calls to the expensive target CNN.

Given the two images to compare, our difference detector can also use one of several *difference metrics* between them. In particular, we have implemented Mean Square Error (MSE), Normalized Root Mean Square Error (NRMSE)⁴, Peak Signal to Noise Ratio (PSNR) and Sum of Absolute Differences (ABSDIFF). The “right” choice of metric again depends on the video—for example, an outdoor video where light levels change during the day will require a normalized metric such as NRMSE. Similarly, the right *firing threshold* for the metric (the difference in metric at which we say that the two frames differ), which we will denote δ_{diff} , also depends on the video and the query. For example, a lower MSE threshold might be needed to detect light objects against a light background than dark ones.

For each of the metrics, NOSCOPE can also run either a comparison on the whole image or a *blocked* comparison where we divide the image into a grid and compute the metric on every grid block. In the blocked version, the system then trains a logistic regression classifier to weigh each block differently when evaluating whether two images are different. The blocked version is more expensive to compute, but it is useful when part of the image does not contain relevant information. For example, in a street view, the signal will change colors frequently but this is not useful for detecting cars.

While different methods performed differently across our datasets, we found that MSE and blocked MSE were generally within a few

⁴ This is a metric that first normalizes the color values within each image and then computes Mean Square Error, which is useful to match similar frames in changing lighting conditions.

percent of the best method, so we only used MSE and blocked MSE to simplify our analysis.

Finally, the difference detector also has a configurable time interval t_{skip} that calculates how often to perform a difference check. For example, in a 30 fps video, it may be reasonable to only test for differences every 15 frames, if the objects of interest are normally in the video much longer than a second. This parameter directly creates a tradeoff between accuracy and speed.

As may be apparent from the examples, various configurations of the difference detector will give varying tradeoffs between execution speed, false positive rate and false negative rate depending on the video stream and query in question. NOSCOPE’s optimizer, described in Section 6, selects and adjusts the difference detector automatically based on frames labeled using the expensive target CNN to navigate this tradeoff space.

5. SPECIALIZED MODELS

The second key technique in NOSCOPE is specialized models. The machine learning community has made stunning advances on benchmarks such as ImageNet [67] a few percentage points at a time by training larger and deeper models on more and more data. These models have naturally been costly to execute. However, small CNNs have also often performed well on most images, and all classification CNN models naturally output a *confidence* in their classification too. Moreover, in query systems such as NOSCOPE, we are generally only interested in identifying *one class* of object in the data. Can we use confidence values to take a small CNN’s output for this class directly when it is confident, and defer to a larger, more accurate model when it is not?

NOSCOPE implements this technique by training a small, specialized CNN for each stream and query using the output from the large target CNN as labels. We implemented CNNs inspired by the AlexNet architecture [44] (filter doubling, dropout), using ReLU units for all the hidden layers and a softmax unit at the end to return a confidence for the class we are querying. However, our networks are significantly more shallow than AlexNet to reduce computational cost. As with difference detectors, we varied several parameters of the specialized models: number of convolutional layers (2 or 4), number of convolution units in the base layer (32 or 64), and number of neurons in the dense layer (32, 64, 128 or 256). NOSCOPE’s optimizer selects the best performing model for each video stream and query, because, as with the difference detectors, these models provide different tradeoffs between speed and accuracy.

Beyond selecting a model, NOSCOPE also selects two thresholds on its confidence value c : c_{low} is the threshold at below which we output 0 as a label (no object in frame), and c_{high} is the threshold above which we output 1 (object detected). For output values of c between c_{low} and c_{high} , NOSCOPE calls the full target CNN on the frame.

Note again that the choice of threshold combines with the choice of model to determine speed and accuracy. For example, a specialized CNN with many layers and convolution units might be much more accurate (resulting in a smaller $[c_{\text{low}}, c_{\text{high}}]$ interval where we call the target CNN), but might be more expensive to compute per frame. Thus, in some cases, we should choose the less accurate CNN that passes more frames to our full model but is faster to evaluate on most input frames.

Finally, to train small CNNs, we use standard CNN training best practices. We divide the input data into a training set and a cross-validation set. Training is done using RMSprop [39] for 1-5 epochs, with early stopping if the training loss increases. We also use early stopping for cross validation. Finally, when selecting between the multiple supported models (a step that is done by the NOSCOPE

optimizer), we use a separate evaluation set that is not part of the training and cross-validation sets for each model.

As discussed in our Evaluation, specialized models trained using a large model such as YOLOv2 perform well empirically on many datasets. By setting c_{low} and c_{high} appropriately, NOSCOPE can often eliminate 90% of frames without calling the full target model and still preserve its accuracy. We also show that training these small models on *scene-specific data* (frames from the same video) leads to better performance than training them on generic object detection datasets.

6. COST-BASED OPTIMIZER

NOSCOPE brings difference detectors and model specialization together using a cost-based optimizer that can efficiently find a good combination of models (e.g., MSE versus PSNR difference detector) and thresholds (δ_{diff} , c_{low} and c_{high}). The optimizer takes in a dataset of images as well as *target accuracy values*, FP* and FN*, that are the desired upper bounds on false positive rate and false negative rate respectively. Formally, the optimizer solves the following problem:

$$\begin{aligned} & \text{maximize} && E(\text{throughput}) \\ & \text{subject to} && \text{false positive rate} < \text{FP}^* \\ & && \text{and false negative rate} < \text{FN}^* \end{aligned}$$

This problem is similar to traditional cost-based estimation planning for user-defined functions [20] and streaming filters [8, 9], but we must also actually perform cost estimation of each candidate filter and set several model-specific parameters for each of them *together* to achieve a target accuracy goal. That is, our problem is not simply a matter of ordering a set of commutative filters, but also requires learning the filters and setting their parameters together to achieve an overall accuracy.

To solve this problem, we use a combination of combinatorial search for model architectures and efficient linear sweeps for the firing thresholds δ_{diff} , c_{low} and c_{high} . The optimizer only considers plans involving up to one difference detector and one specialized model, because we found that stacking more such models did not help significantly. For such plans, the optimizer can explore the *complete* space of combinations of difference detectors and specialized models within several seconds, at a negligible cost compared, for example, to labeling all the input data using a full CNN such as YOLOv2. We now describe the key components of the optimizer.

6.1 Input Data Preparation

The optimizer executes on an input dataset of frames labeled by the full target CNN. For example, such a set could be obtained in the first few days of a new stream, and maintained using reservoir sampling thereafter. The optimizer begins by splitting the input data into a *training set* and an *evaluation set* that will only be used for model selection (otherwise, training specialized models or even the simpler models in the difference detector on the same data used for evaluation could lead to overfitting). The data is split at the level of large contiguous blocks of time so that frames in the evaluation set are temporally far away from those in the training set (otherwise, every possible image would essentially appear in both sets if there is temporal locality in the video, eliminating the opportunity to test for overfitting).

6.2 Cost Model

The output of the optimizer will eventually be a configuration of difference detector and specialized model to use (or the decision not to use one of these). For any such configuration, the optimizer estimates its execution time per frame using the pass-through rates

of the detector and specialized model in question on the training data, and static measurements of the execution time of each model on the user’s hardware. For example, consider a configuration with the following two filters:

1. A Mean Squared Error (MSE) difference detector that is configured to check frames every t_{skip} seconds and fire if the frame’s MSE with a reference image is higher than δ_{diff} .
2. A two-layer CNN with 64 convolutional units and 64 neurons in the dense layer, configured with detection thresholds c_{low} and c_{high} .

The cost model determines the expected time per frame by first measuring what fraction of frames remain after the skipping done by t_{skip} ; call this fraction f_s . Next, it computes the fraction of these frames in the training data that pass the MSE filter, f_m . Finally, it computes the fraction of these difference detector passing frames whose confidence under the specialized CNN lies between c_{low} and c_{high} – call this f_c . The expected execution time per frame is then

$$f_s T_{\text{MSE}} + f_s f_m T_{\text{SpecializedCNN}} + f_s f_m f_c T_{\text{FullCNN}}$$

where T_{MSE} , $T_{\text{SpecializedCNN}}$ and T_{FullCNN} are the execution times per frame for the MSE filter, specialized CNN and target model CNN respectively. These execution times are data-independent so they can be measured once when the system is installed on a hardware platform.

6.3 Search Algorithm

There are three major challenges to searching for an optimal configuration. First, filters may be complex and exhibit non-linearity with respect to the cascade architecture and input parameters; for example, their selectivities will not be known a priori. Second, filters are not independent (cf. [9]): one specialized model may complement one difference detector but not another, and the viable combinations of thresholds for each pair of filters will differ across scenes. Third, the full search space for filter configurations is very large because the firing thresholds δ_{diff} , c_{low} and c_{high} are continuous values.

We address these challenges via a three-stage process. First, we train each filter individually on our training set. Second, we examine the behavior of each filter in isolation to determine how it will score each frame. Finally, we explore all combinations of a difference detector and a specialized models and use an efficient linear sweep of the viable combinations of thresholds to determine the lowest-cost way to combine these models. In more detail, NOSCOPE’s search proceeds as follows:

1.) Train filters: First, we train instances of each of our model-based filters (e.g., specialized CNNs and logistic regression based blocked difference detectors) on the training data. For the CNNs, we consider a grid of combinations of model architectures (e.g., 2 or 4 layers, 32 or 64 convolutional units, etc). In our current implementation, this leads to about 20 distinct configurations of models. When training these models, we further subdivide the original training data to create a cross-validation set that is not part of training, a standard practice when training CNNs.

2.) Profile individual filters: Next, we perform selectivity estimation by profiling individual filters on our evaluation set (the input data that the optimizer set aside at the beginning for evaluation) to determine their selectivity and sensitivity. These quantities are difficult to infer beforehand because they depend significantly on the video, so we run each of the trained filters on every frame of the evaluation set. We then log the score that the filter gives to each frame (e.g., Mean Square Error or specialized CNN output

confidence), which will then be used to set the thresholds δ_{diff} , c_{low} and c_{high} .

3.) Examine filter combinations: Filter parameters are *not* independent because the thresholds for a pair of filters may influence one another and therefore need to be set together. For example, if we use MSE as our difference detection metric, the threshold δ_{diff} that we set for difference detection directly affects which *frames* are passed to the downstream specialized CNN and which *thresholds* c_{low} and c_{high} we can set for it (e.g., if the difference detector already forces a lot of false negatives, we need to be more conservative in the CNN).

We solve the problem of dependencies in filter selection via an efficient algorithm to sweep feasible combinations of thresholds. Specifically, for each difference detector D , we first sort the frames of the training data in decreasing order of the detector’s difference metric (δ). This yields a list of frames L_D where we can easily sweep through firing thresholds δ_{diff} . Next, we compute, for each prefix of the list L_D , how many frames would be false positives and false negatives if we set δ_{diff} at that threshold (i.e., frames that we will mislabel due to the difference detector not firing).

Next, for each specialized CNN, C , we examine the list of frames L_D in discrete intervals (e.g., one step for every percentile of the list) and keep track of the list of frames in that prefix of L_D sorted by their confidence level under C , c_C . Given this list, we can set c_{low} and c_{high} so as to get the desired false positive and false negative rates FP^* and FN^* : start with these thresholds at the extreme (0 and maximum confidence), then move c_{low} up until the false negative rate of the combined difference detector and CNN reaches FN^* , and move c_{high} down until the combined false positive rate reaches FP^* . Finally, for each such configuration of detector D , CNN C , δ_{diff} and resulting c_{low} and c_{high} , we compute the expected throughput using our cost model (Section 6.2) and output the best result.⁵

Running Time. The overall complexity of this algorithm is $O(n_d n_c n_t)$, where n_d is the total number of difference detector configurations considered, n_c is the total number of specialized model configurations, and n_t is the total number of firing thresholds considered during the sweep down L_D . In addition, we need to run each of the n_d difference detectors and n_c specialized model configurations on the training data once (but not each *pair of filters* together). Overall, the running time of the algorithm is often just a few seconds because each of n_d , n_c and n_t is small (less than 100). Moreover, even training and applying the specialized models we will test is faster than obtaining the “ground truth” labels for the training data using a full-scale CNN like YOLOv2. As we show in Section 9.3.3, all steps of the optimizer together run faster than labeling the data using YOLOv2.

7. IMPLEMENTATION

We implemented NOSCOPE using a combination of C++ and TensorFlow for the “data plane” operators and Python for the optimizer. We invested significant effort to optimize the data plane to achieve maximum performance for our difference detectors and specialized models; the code is open-sourced and available online⁶. In particular, we parallelize many of the CPU-intensive operations over multiple cores, use vectorized libraries where possible, and batch data for computations on the GPU. These optimizations make a large difference in performance for many configurations of NOSCOPE because the bulk of the video frames are eliminated by the

⁵ In this search above, we also consider the “null” difference detector and CNN to allow disabling one of the components.

⁶ <https://github.com/stanford-futuredata/tensorflow-noscope/tree/noscope>, <https://github.com/stanford-futuredata/noscope>

difference detector and specialized CNN.

At a high level, NOSCOPE’s data plane runs the following steps: 1) load the incoming video frames into memory, 2) run a difference detector, 3) run a specialized CNN on the frames that pass the difference detector, and 4) run a target model such as YOLOv2 on the frames that are not confidently labeled by the specialized CNN. We next describe each of these steps in turn.

Loading Video. NOSCOPE can load video frames either directly from memory from the `ffmpeg` and `libav` libraries for video decoding. After loading frames, it resizes them for downstream processing if needed using `OpenCV` (CNNs such as YOLOv2 require a specific size for input images, such as 416x416 pixels).

Difference Detectors. We implemented difference detectors such as Mean Squared Error (MSE) using multithreaded CPU code via `OpenCV`. For some of the filters, we also wrote hand-tuned C++ code to fuse together the operators required. For example, MSE requires computing the expression $\sum((a - b)^2)$, where a and b are two images, which would require materializing $a-b$ in memory using `OpenCV`’s standard array operators. Instead, we wrote a new operator to compute it directly given arrays a and b . Finally, we parallelized the difference detector at the level of frames—that is, we process multiple decoded frames in parallel using different threads.

For the blocked difference detectors that use logistic regression to weigh different portions of the image differently, we used `scikit-learn` in the training phase to set their weights. We then evaluate the resulting logistic regression models at runtime using C++ code.

Specialized Models. We trained our specialized CNNs using `TensorFlow`. As discussed in Section 5, we used standard best practices for CNN training such as cross-validation and early stopping, and our optimizer selects which CNN to run using an evaluation set that is distinct from the training data.

During evaluation, we evaluate the specialized CNNs on the GPU using `TensorFlow`’s C++ interface. Because the cost of communicating with the GPU is high, we batch input images before passing them to the GPU.

Finally, a key pre-processing step for both CNN evaluation and training is to mean-center the pixel values and change the dynamic range in each color channel to $[-1, 1]$. We implemented this step on the CPU using `OpenCV` and multithreading in a similar manner to difference detection.

Running the Target Model. We used YOLOv2 [65] as our target model and applied it on frames in batches, similar to the way we apply `TensorFlow`. We pre-load the YOLOv2 CNN onto the GPU and keep it in memory across evaluations to avoid reloading this large model.

Optimizer Implementation. Our optimizer is written in Python, and calls our C++ code for difference detectors and CNNs when obtaining training data. As described in Section 6, the cost of the optimizer itself is relatively small. The bulk of the runtime is spent training the specialized CNN models on its input data.

8. LIMITATIONS

Although NOSCOPE’s approach can significantly accelerate CNN-based video processing, we wish to point out several limitations. We designed the current system primarily for the task of object classification in fixed-angle video (e.g., traffic cameras), which we believe represents an important subset of all video data processing.

Fixed-Angle Video. Our current difference detectors only work on video shot by static cameras, and our results for specialized CNNs

Video Name	Object	Resolution	FPS	# Frames	Length (hrs)
night-street	car	1420x1080	30	648k	6.0
store	person	1170x1080	30	864k	8.0
roundabout	car	1280x720	25	1067k	11.9
coral	person	1280x720	30	648k	6.0
elevator	person	640x480	30	901k	8.3
amsterdam	car	680x420	30	371k	3.4
taipei	bus	1000x570	30	648k	6.0

Table 1: Video streams and object labels queried in our evaluation.

are also obtained on fixed-angle videos. The video processing community has also developed techniques to track objects when the camera is moving [56], so these techniques present a promising approach to extend NOSCOPE to moving cameras.

Binary Classification Task. We have only designed and evaluated NOSCOPE for binary classification of objects in one object class from the target CNN (e.g., finding all frames with people, or all frames with cars, or all frames with buses, etc.). It would be natural to extend this type of system to more complex queries involving objects of multiple classes, localization (not just “does the frame contain a person” but “where is the person in the frame”), and counting queries (“how many people are in the frame”). Some complex queries could be handled by ANDing or ORing the results of binary classification queries (e.g., “does the frame contain a dog AND no human”), but others will require new forms of difference detectors and specialized CNNs.

Model Drift. Our current implementation assumes that the training data passed to NOSCOPE’s optimizer is from the same distribution as the subsequent video observed. If the scene changes dramatically after a certain point of time, NOSCOPE needs to be called again to re-optimize for the new data distribution. Likewise, if the scene changes periodically during the video (e.g., by cycling between day and night), the training data needs to contain frames representative of all conditions. While this limitation would be interesting to address automatically by tracking model drift, we believe that it is acceptable for many fixed-angle camera scenarios, such as traffic or security cameras, which observe a similar scene over a period of months or years. For these types of videos, a sample of training data spread throughout the year should be sufficient to produce good training data for a model that can be applied continuously.

Image Batching. Our implementation batches together images passed to the GPU for speed. While this is acceptable for historical video that is available all at once, it can introduce a short delay for live video, proportional to the number of frames batched. For example, batching together 100 frames at a time in a 30 fps video can add a delay of up to 3.3 seconds. Alternatively, a system monitoring 100 streams would be able to simply batch together data from different streams, applying different CNN models to each one, allowing a range of optimizations [55] we have not yet explored in the context of streaming video.

9. EVALUATION

This evaluation answers the following question: how does NOSCOPE perform on the binary classification task for real world surveillance videos? In sum, we find that:

1. NOSCOPE achieves 40-3200× higher throughput (i.e. frames processed per second) than state-of-the-art CNN implementations while maintaining 99% of their accuracy, and 100-7300× higher throughput while maintaining 90+% accuracy.
2. The (mis)configuration of filters dramatically affects the over-

all performance of NOSCOPE. Moreover, the optimal configuration parameters for filters on one video stream will almost always provide poor performance if used for filters on another video stream.

3. NOSCOPE’s cost-based optimizer consistently sets filter parameters that provide large performance improvements subject to user defined accuracy constraints. Difference detection filters and specialized model filters improve the throughput on average by $3\times$ and $80\times$ respectively.
4. *Scene-specific* specialization of models to a particular video stream provides a $1.25\text{--}25\times$ improvement compared to models trained for the detection task across multiple environments.

9.1 Experimental Setup

Evaluation Task and Datasets. We evaluated the accuracy of NOSCOPE on the binary classification task compared to a state-of-the-art CNN based object detector, YOLOv2 [65]. Accuracy is measured by comparing frames labeled by each system in 30 frame windows. For a window to be considered “labeled correctly”, both systems must agree on the presence of the target object in 28 of the 30 frames in a window. We use this somewhat permissive accuracy measure because YOLOv2 frequently fails to label objects clearly visible in the frame, unfairly penalizing NOSCOPE’s correct labels.

For throughput measurements, we timed the complete end-to-end system excluding the time taken to decode video frames (note: we report throughput as frames processed per second). We omit video decode times for three reasons. First, it is standard to omit video decode time in computer vision [15, 64–66]. Second, both GPUs and CPUs can decode video at a high rate because of built-in hardware decoders [61]. For example, on our Tesla P100, we measured 4000 fps when decoding 400x400 H.264 video and 5600 fps when decoding 400x400 MPEG; some processors even have multiple decoders. Third, for some visual sensors, we can directly obtain a raw stream of frames from the hardware.

Table 1 lists the video datasets and target objects used in our evaluation. The first 250,000 frames (roughly 2.3 hours) of each dataset was reserved for training and model selection in NOSCOPE’s query optimizer; the remainder (1-9 hours) was used for testing to measure throughput and accuracy by our metrics. Two examples are shown in Figure 4.

Hardware Environment. We performed our experiments on an NVIDIA DGX-1 server, using at most one Tesla P100 GPU and 32 Intel Xeon E5-2698 v4 cores during each experiment. The complete system had 80 cores and multiple GPUs, but we limited our testing to a subset of these so our results would be representative of a less expensive server. The system also had a total of 528 GB of RAM.

Target CNN. We used YOLOv2 [65], a state-of-the-art multi-scale CNN, as NOSCOPE’s target CNN. YOLOv2 operates on 416x416 pixel images (resizing larger or smaller images when necessary). YOLOv2 achieved 80 fps on the Tesla P100 GPU installed on our measurement machine.

9.2 Overall Performance

Figure 5 shows the overall range of performance that NOSCOPE achieves on our datasets. We plot this through a speedup vs. accuracy tradeoff curve, where speedup is the speedup over YOLOv2, and accuracy is the percent of correctly labeled time windows in the binary classification task. For each dataset, we obtained the points in the plot by running our optimizer with increasing false positive and false negative thresholds (FP^* and FN^*) and measuring the resulting speedup.

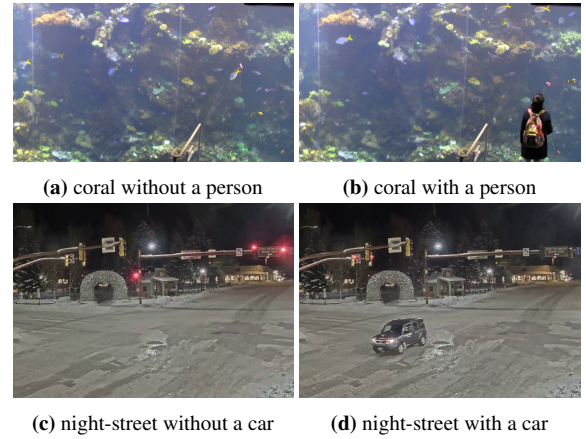


Figure 4: Examples of the datasets, with and without the object of interest.

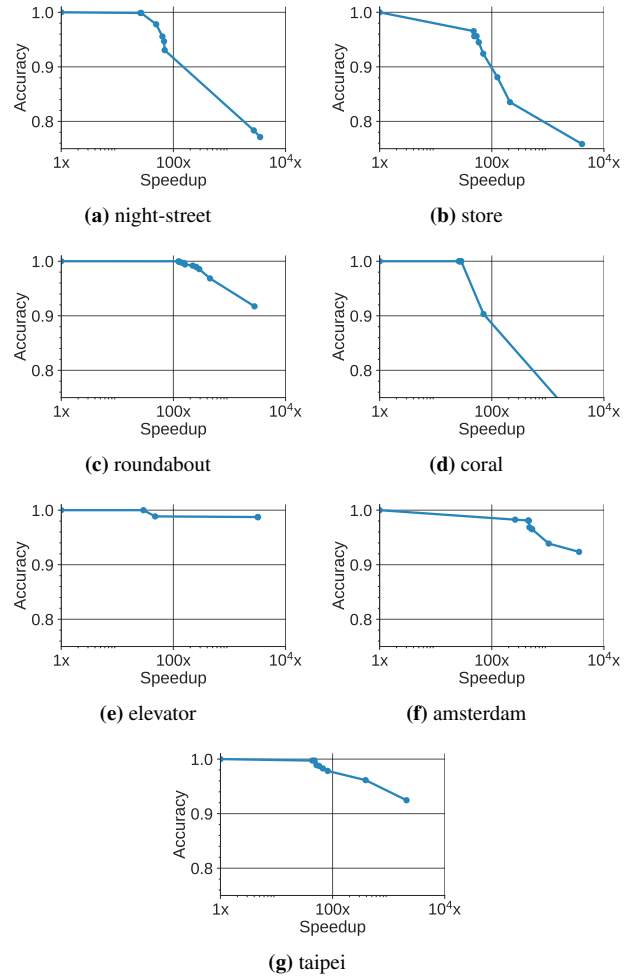


Figure 5: Accuracy vs. speedup curves achieved by NOSCOPE on each dataset. “Accuracy” here means the percent of correctly labeled time windows in the binary classification task, and “speedup” is over YOLOv2.

NOSCOPE can achieve several orders of magnitude speedup across all the datasets depending on the desired accuracy levels. In all cases, NOSCOPE achieves a $30\times$ speedup with at least 98% accuracy (note that because YOLOv2 itself ran at 80 fps on our hardware, this is $80\times$ real time). In many cases, this level of accuracy is retained even for a $100\times$ speedup, and NOSCOPE can get $1000\times$

to $10,000\times$ speedups at 90+% accuracy. The video with the lowest peak speedup at the 90% accuracy mark is coral, which shows an aquarium with moving fish, where the difference detectors cannot eliminate many frames; even in this video, however, NOSCOPE can offer a $30\times$ speedup over YOLOv2 with no loss in accuracy.

9.3 Impact of Optimizer

In this section, we explore how much impact the decisions of NOSCOPE’s optimizer have on performance. We begin by showing that the filter types and thresholds chosen by the optimizer differ significantly across videos based on their characteristics. We also show that choosing other settings for these parameters would greatly decrease speed or accuracy in many cases, so parameters cannot simply be transferred across videos.

9.3.1 Configurations Chosen Across Datasets

Table 2 shows the difference detectors, specialized models, and detection thresholds chosen by the optimizer across our sample datasets when we set a 1% target false positive and false negative rate. We observe that these are substantially different across videos, even when the optimizer selects the same filter class (e.g., difference detection based on MSE on the whole image). We make a few observations about these results:

First, the best-performing difference detectors in these seven videos are based on Mean Squared Error (MSE), which was slightly more effective than other metrics we explored such as normalized MSE and PSNR. However, the best specific types of MSE chosen depend on the video. For example, coral and store are scenes with a dynamic background (e.g., coral shows an aquarium with colorful fish swimming in the background, and NOSCOPE is asked to detect people that look at the fish). In these scenes, computing MSE against several frames past instead of against a single “empty” reference frame is more effective.

Second, the thresholds chosen differ significantly as well. For example, for difference detection, taipei has a high threshold because there is a lot of small-scale activity in the background, but the objects we wish to detect, buses, are generally large and cause a difference in more of the frame. The upper and lower thresholds for CNNs also vary even across the same target object class, partly due to varying difficulty in detecting the objects in different scenes. For example, in some videos, the c_{low} threshold for declaring that there is no object in a frame is extremely low because increase it would lead to too many false negatives.

Third, the best specialized model architectures also varied by video and query. In particular, we found that in many videos, the larger CNNs (with 4 layers or with more convolutional units and dense layer neurons) would overfit given the fairly small training set we used (150,000 frames out of the 250,000 frames set aside for both training and evaluation). However, the best combination of these parameters varied across videos, and NOSCOPE’s training routine that selects models based on an unseen evaluation set automatically chose an accurate model that did not overfit.

9.3.2 Non-Transferability Across Datasets

Because the best-performing filter configurations varied significantly across datasets, transferring parameters from one dataset to another also leads to poor performance. In this section, we show two results illustrating this.

Specialized Model Architectures. We tried using the specialized model architecture⁷ from night-street (a CNN with parameters $L=2, C=16, D=128$) on the taipei dataset (whose optimal CNN had

⁷ Note that we transferred only the *architecture*, not the learned model from each dataset. We trained a new model with each archi-

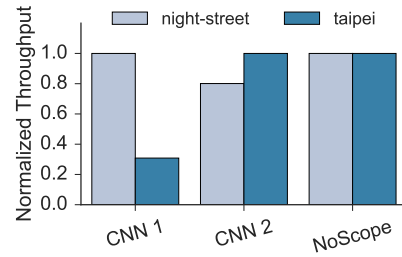


Figure 6: Normalized performance of NOSCOPE with two different specialized CNN models on the night-street and taipei videos. We see that choosing a different CNN architecture for each video, even though this architecture performed well on another dataset, reduces throughput. NOSCOPE automatically selects the best-performing CNN.

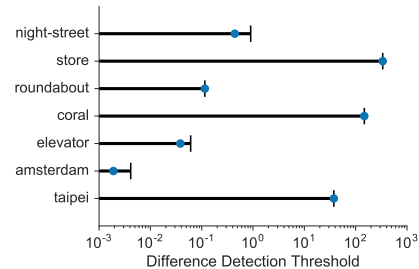


Figure 7: Firing thresholds δ_{diff} chosen by the optimizer for each video (blue dots), along with the range of thresholds that can achieve 1% false positive and false negative rate for that video (black lines).

$L=2, C=64, D=32$), and vice-versa. Although these architectures have similar properties (e.g., two layers), they required significantly different parameters to achieve our 1% target false positive and false negative rates on each dataset. This resulted in a $1.25\times$ to $3\times$ difference in throughput for the overall NOSCOPE pipeline, as shown in Figure 6.

Detection Thresholds. We also plotted the range of feasible thresholds for the difference detector (δ_{diff}), as well as the actual threshold chosen, in Figure 7. “Feasible” thresholds here are the ones where the system can stay within the 1% false positive and false negative rates we had requested for the optimizer. Beyond a certain upper limit, the difference detector alone will introduce too many incorrect labels. As we see in the plot, the range of values for each video is different and the best-performing threshold is often near the top of this range. Thus, any attempt to use a common threshold between videos would either result in not meeting the accuracy target (if the threshold is too high) or lower performance than the threshold NOSCOPE chose (if the threshold is too low).

9.3.3 Running Time of Optimizer

We measured the time it takes to run our optimizer across several datasets, showing the most time-consuming one in Figure 8. In all cases, initializing NOSCOPE requires labeling all the frames in the training data with YOLOv2, followed by training all supported specialized models and difference detectors on this data, then selecting a combination of them using the algorithm in Section 6. As shown in the figure, YOLOv2 application takes longer than all the other steps combined, meaning that NOSCOPE’s optimizer could run in real time on a second GPU while the system is first observing a new stream. Training of the specialized CNNs takes the next longest

Video Name	Difference			SCNN (L)	SCNN (C)	SCNN (D)	C_{low}	C_{high}
	Detector (DD)	DD (R)	δ_{diff}					
night-street	global MSE	reference	0.441	2	16	128	2.20E-7	0.176
store	blocked MSE	previous	336.7	2	32	128	0.0100	0.998
roundabout	global MSE	reference	0.115	4	32	32	0.0741	0.855
coral	blocked MSE	previous	147.3	2	16	128	0.00613	0.998
elevator	global MSE	reference	0.0383	2	32	256	0.00401	0.517
amsterdam	global MSE	reference	0.0019	2	64	256	0.128	0.998
taipei	global MSE	reference	37.5	2	64	32	0.114	0.994

Table 2: Filter types and thresholds chosen by NOSCOPE’s optimizer for each video at 1% target false positive and false negative rates. We observe that both the filter types (e.g., global or blocked Mean Square Error versus either a reference frame or the previous frame, denoted R) and their thresholds (e.g., the difference in MSE that is considered significant, or the upper and lower detection thresholds for the specialized models) vary significantly across videos. For the specialized models (denoted SCNN), L denotes the number of layers, C the number of convolutional units, and D the dimension of the dense layers.

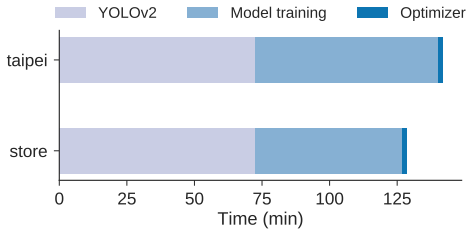


Figure 8: Breakdown of training and optimization time on taipei dataset. Passing all the training frames through YOLOv2 to obtain their true labels dominates the cost, followed by training all variants of our specialized models and then the rest of the steps in the optimizer.

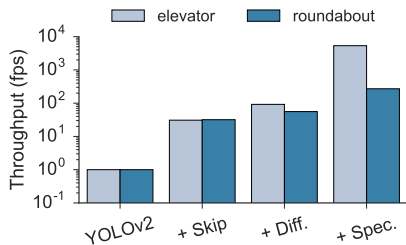


Figure 9: Factor analysis showing the impact of adding frame skipping, difference detection and specialized models on two videos. From left to right, we add each of these filters in turn over YOLOv2 and show the normalized throughput on a logarithmic scale.

amount of time; in this case, we trained 20 different models. Note that we have not heavily optimized this step or tried to reduce the search space of models yet, so it may be possible to improve it.

9.4 Impact of Individual Filters

To analyze the impact of each of our filters on NOSCOPE’s performance, we ran a factor analysis and lesion study on two videos, with results shown in Figures 9 and 10.

In the factor analysis, we started by running all frames through YOLOv2 and gradually added three filters: frame skipping (which is usually part of our difference detector operators but was separated here to show that skipping alone does not provide the full benefit), difference detection on the skipped frames, and finally specialized model evaluation. The specific pipeline of filters we show was selected to achieve 1% false positive and false negative rates on the videos using NOSCOPE’s optimizer. We see that each filter adds a nontrivial speedup (the smallest is from difference detection over skipping, but even that is $1.8\times$ for roundabout and $3\times$ for elevator).

In the lesion study, we also tried removing just one element

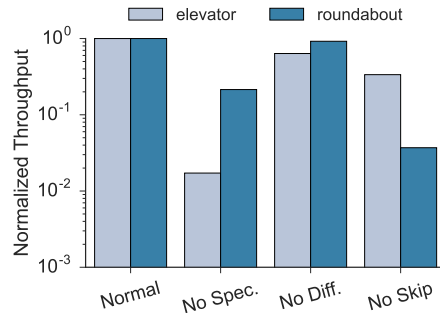


Figure 10: Lesion study showing the impact of removing each of specialized models, difference detection and frame skipping on two videos. The leftmost bars show normalized performance with all of NOSCOPE’s features enabled, and bars to the right show the effect of removing each filter on its own.

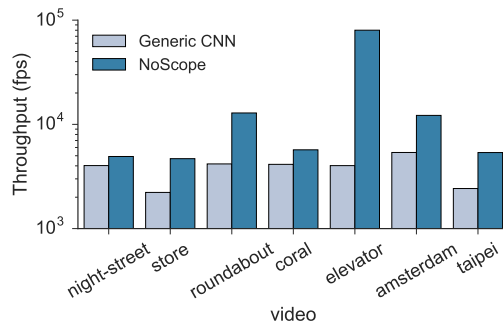


Figure 11: Throughput, Generic CNN vs. NOSCOPE. Substituting the specialized CNN model in NOSCOPE with an equivalent model trained on MS-COCO (a general-purpose training set of images used by YOLOv2) results in a decrease in the end-to-end throughput of the system across all videos.

at a time from the complete NOSCOPE pipeline. As before, we started with a pipeline configured to achieve 1% false positive and false negative rates. As shown in Figure 10, each element again contributes to the overall throughput of the pipeline, showing that NOSCOPE’s filtering techniques are all important to its performance.

9.5 Impact of Scene Specialization

Finally, we wanted to evaluate the benefit of our *scene-specific* model specialization technique (Section 5) over training on general computer vision datasets. Our hypothesis in designing NOSCOPE was that we can achieve much higher accuracy by training models on past frames from the *same video* to leverage the characteristics of that particular scene (e.g., fixed perspective on the target object, fixed range of scales for objects observed, fixed background, etc.).

To evaluate this hypothesis, we trained three models (using similar architectures to what NOSCOPE uses) for binary classification (on the classes of objects we evaluate NOSCOPE on: people, buses, and cars) on the more general MS-COCO dataset [49], a recent high-quality object detection dataset. For each class of objects, the best model was selected and was run through our pipeline. Figure 11 shows the resulting throughput across our videos. In all cases, the specialized models trained by NOSCOPE outperform the generic model of the same size trained on MS-COCO, showing that scene-specific specialization does indeed improve the accuracy of small models.

10. RELATED WORK

NOSCOPE builds on a long tradition of data management for multimedia and video and upon recent advances in computer vision, machine learning, computer architecture, and data processing. We outline several major related thrusts below:

Model Compression and Distillation. To reduce the size and the evaluation time of CNNs, various efforts have proposed techniques for model compression (alternatively, distillation): producing a smaller, equivalent model from a larger model. One strategy for model compression is to use the behavior of a larger model (e.g., its output confidences) to train a smaller model, either distilling an ensemble of models into a smaller model [14], or distilling one large network into one smaller network [7, 40]. One can think of this form of distillation as an instance of transfer learning [59], where one model’s “knowledge” is “reused” in another to boost accuracy. Another strategy is to modify the network weights directly, either via hashing [21] or pruning and literal compression (e.g., quantization) of the weights themselves [36, 62]. These networks are almost always more amenable to hardware acceleration—a related line of research [37, 63]. The key difference between this related work and our model specialization method is that this related work is designed to produce smaller models preserve the full *generality* of the large model: that is, the small model can perform all of the tasks as the large model, without loss in accuracy for any of them. In contrast, NOSCOPE explicitly *specializes* CNNs that were trained on a large variety of input images and target objects to instead operate over a specific video stream with a smaller number of target objects; this query-aware specialization is key to improving performance.

Model Specialization. We are not aware of any other work accelerating CNN inference time via task specialization on video. However, related strategies for specialization have been shown to boost *accuracy* (but not runtime) [52, 54], and there are a range of models designed for detecting specific classes of objects in video. One of the most popular video-based object detection tasks is pedestrian detection [13, 25], with a range of CNN-based approaches (e.g., [69]). In NOSCOPE, our goal is to specialize to a *range* of inputs automatically, using a large general CNN as guidance. We evaluate a handful of different labels based on available datasets, but theoretically any of the 9000 classes recognized by CNNs today could be specialized.

Model Cascades. The concept of combining a sequence of classifiers to improve runtime performance is known as a *cascade*; of the first such cascades is the Viola-Jones detector [73], which uses a cascade of traditional image processing features. If any classifier is confident about the output, the cascade short-circuits evaluation, thus improving execution speed. Recent work has focused on learning cascades for pedestrian detection [16] and facial recognition [48, 70] *image* tasks. In NOSCOPE, we design a cascade architecture for use in *video*, specifically adapted to account for temporal locality (via difference detectors) and scene- and label-specific locality (via

model specialization). In another related line of work, several CNNs specialized for video take multiple frames as input to improve accuracy [28, 74], but again, this work focuses on accuracy, not on evaluation speed like NOSCOPE. Finally, NOSCOPE’s use of a cost-based optimizer to select between different filters and different thresholds for each filter based on the video stream and a reference CNN is novel compared to work in the computer vision literature that uses the same sequence of filters (or that optimize solely for accuracy, not computational cost; cf. [72]). In this way, NOSCOPE acts as a model selection tool [12, 22] but is inspired by conventional database cost optimization [68] and related efforts [19, 41] on self-adapting query processing engines.

ML Model Management and Stream Processing Systems. While have provided an overview of related multimedia query engines (e.g., [6, 30, 47, 57, 80]) in Section 2 and a comparison with several filter- and UDF-based query processors in Section 6, NOSCOPE also draws inspiration from a number of recent machine learning model management systems. Velox [23] provides a high-performance platform for serving personalized models at scale, while MLBase [43] provides a declarative interface for specifying modeling tasks, and MacroBase [10, 11] provides a platform for executing classification and data aggregation tasks on fast data. Similarly, a range of systems from academia and industry provide stream processing functionality [4, 17, 24, 33]; here, we specifically focus on video stream processing. Like Bismarck [29], NOSCOPE is structured as a sequence of dataflow operators, but for performing video classification. Of these previous systems, MacroBase is the most closely related; however, in NOSCOPE, we focus specifically on video classification and develop new operators and a cost-based optimizer for that task. Looking forward, we are eager to integrate NOSCOPE’s classifiers into MacroBase and similar systems.

11. CONCLUSIONS

Video is one of the richest and most abundant sources of data available. At the same time, convolutional neural networks (CNNs) have dramatically improved our ability to extract semantic information from video. However, naïvely applying CNNs is prohibitively expensive for large-scale video data management systems. To solve this problem, we have presented a cost-based optimizer that can automatically select a set of filters to accelerate labeling an individual video stream while retaining accuracy. Our prototype system, NOSCOPE, achieves speedups of up to 120-3,200× while retaining 95-99% accuracy on real-world video streams. These results indicate that, for binary classification on fixed-angle video streams, state-of-the-art object labeling techniques can be applied on large datasets at several orders of magnitude lower computational cost.

Acknowledgments

We thank the many members of the Stanford InfoLab for providing feedback on this work. This research was supported in part by Toyota Research Institute, Intel, the Army High Performance Computing Research Center, RWE AG, Visa, Keysight Technologies, Facebook, VMWare, and Philips Lighting. As NOSCOPE is open source and publicly available, there is no correspondence—either direct or implied—between the use cases described in this work and the above institutions that supported this research.

12. REFERENCES

- [1] Typical cnn architecture. Creative Commons Attribution-Share Alike 4.0 International, Wikimedia Commons.
- [2] Cisco VNI forecast and methodology, 2015-2020. Technical report, 2016.
- [3] 2017. <https://fortunelords.com/youtube-statistics/>.

- [4] D. J. Abadi et al. The design of the Borealis stream processing engine. In *CIDR*, 2005.
- [5] W. Aref, M. Hammad, A. C. Catlin, I. Ilyas, et al. Video query processing in the VDBMS testbed for video database research. In *ACM-MMDB*, 2003.
- [6] F. Arman, A. Hsu, and M.-Y. Chiu. Image processing on compressed data for large video databases. In *ACMMM*, 1993.
- [7] J. Ba and R. Caruana. Do deep nets really need to be deep? In *NIPS*, 2014.
- [8] B. Babcock, S. Babu, M. Datar, R. Motwani, and D. Thomas. Operator scheduling in data stream systems. *VLDBJ*, 13(4):333–353, 2004.
- [9] S. Babu, R. Motwani, K. Munagala, I. Nishizawa, and J. Widom. Adaptive ordering of pipelined stream filters. In *SIGMOD*, 2004.
- [10] P. Bailis, E. Gan, D. Narayanan, S. Madden, K. Rong, and S. Suri. Macrobase: Prioritizing attention in fast data. In *SIGMOD*, 2017.
- [11] P. Bailis, E. Gan, K. Rong, and S. Suri. Prioritizing attention in fast data: Principles and promise. In *CIDR*, 2017.
- [12] M. G. Bello. Enhanced training algorithms, and integrated training/architecture selection for multilayer perceptron networks. *IEEE Transactions on Neural networks*, 3(6):864–875, 1992.
- [13] R. Benenson, M. Omran, J. H. Hosang, and B. Schiele. Ten years of pedestrian detection, what have we learned? In *ECCV*, 2014.
- [14] C. Bucilua, R. Caruana, and A. Niculescu-Mizil. Model compression. In *KDD*, 2006.
- [15] Z. Cai, Q. Fan, R. S. Feris, and N. Vasconcelos. A unified multi-scale deep convolutional neural network for fast object detection. In *ECCV*, 2016.
- [16] Z. Cai, M. Saberian, and N. Vasconcelos. Learning complexity-aware cascades for deep pedestrian detection. In *ICCV*, 2015.
- [17] S. Chandrasekaran et al. TelegraphCQ: Continuous dataflow processing for an uncertain world. In *CIDR*, 2003.
- [18] S.-F. Chang, W. Chen, H. J. Meng, H. Sundaram, and D. Zhong. A fully automated content-based video search engine supporting spatiotemporal queries. *IEEE Transactions on Circuits and Systems for Video Technology*, 8(5):602–615, 1998.
- [19] S. Chaudhuri and V. Narasayya. Self-tuning database systems: a decade of progress. In *VLDB*, 2007.
- [20] S. Chaudhuri and K. Shim. Optimization of queries with user-defined predicates. *ACM Transactions on Database Systems (TODS)*, 24(2):177–228, 1999.
- [21] W. Chen, J. T. Wilson, S. Tyree, K. Q. Weinberger, and Y. Chen. Compressing neural networks with the hashing trick. In *ICML*, 2015.
- [22] Y. Cheng et al. An exploration of parameter redundancy in deep networks with circulant projections. In *ICCV*, 2015.
- [23] D. Crankshaw, P. Bailis, J. E. Gonzalez, H. Li, Z. Zhang, M. J. Franklin, A. Ghodsi, and M. I. Jordan. The missing piece in complex analytics: Low latency, scalable model management and serving with Velox, 2015.
- [24] C. Cranor, T. Johnson, O. Spataschek, and V. Shkapenyuk. Gigascope: a stream database for network applications. In *SIGMOD*, 2003.
- [25] P. Dollar, C. Wojek, B. Schiele, and P. Perona. Pedestrian detection: An evaluation of the state of the art. *Transactions on Pattern Analysis and Machine Intelligence*, 34(4):743–761, 2012.
- [26] J. Donahue, L. Anne Hendricks, S. Guadarrama, M. Rohrbach, S. Venugopalan, K. Saenko, and T. Darrell. Long-term recurrent convolutional networks for visual recognition and description. In *CVPR*, 2015.
- [27] A. Esteva, B. Kuprel, R. A. Novoa, J. Ko, S. M. Swetter, H. M. Blau, and S. Thrun. Dermatologist-level classification of skin cancer with deep neural networks. *Nature*, 542(7639):115–118, 2017.
- [28] C. Feichtenhofer, A. Pinz, and R. Wildes. Spatiotemporal residual networks for video action recognition. In *NIPS*, 2016.
- [29] X. Feng, A. Kumar, B. Recht, and C. Ré. Towards a unified architecture for in-RDBMS analytics. In *SIGMOD*, 2012.
- [30] M. Flickner et al. Query by image and video content: The QBIC system. *computer*, 28(9):23–32, 1995.
- [31] A. Geiger, P. Lenz, and R. Urtasun. Are we ready for autonomous driving? the kitti vision benchmark suite. In *CVPR*, 2012.
- [32] S. Gibbs, C. Breiteneder, and D. Tsichritzis. Audio/video databases: An object-oriented approach. In *ICDE*, 1993.
- [33] L. Girod et al. Wavescope: a signal-oriented data stream management system. In *ICDE*, 2006.
- [34] I. Goodfellow, Y. Bengio, and A. Courville. *Deep Learning*. MIT Press, 2016. <http://www.deeplearningbook.org>.
- [35] N. Haering, P. L. Venetianer, and A. Lipton. The evolution of video surveillance: an overview. *Machine Vision and Applications*, 19(5):279–290, 2008.
- [36] S. Han et al. Deep compression: Compressing deep neural networks with pruning, trained quantization and Huffman coding. In *ICLR*, 2016.
- [37] S. Han et al. EIE: efficient inference engine on compressed deep neural network. In *ISCA*, 2016.
- [38] K. He, X. Zhang, S. Ren, and J. Sun. Deep residual learning for image recognition. In *CVPR*, 2016.
- [39] G. Hinton and T. Tieleman. Lecture 6.5 - rmsprop. Technical report, 2012.
- [40] G. Hinton, O. Vinyals, and J. Dean. Distilling the knowledge in a neural network. *arXiv preprint arXiv:1503.02531*, 2015.
- [41] S. Idreos, M. L. Kersten, S. Manegold, et al. Database cracking. In *CIDR*, 2007.
- [42] R. Jain and A. Hampapur. Metadata in video databases. In *SIGMOD*, 1994.
- [43] T. Kraska et al. Mbase: A distributed machine-learning system. In *CIDR*, 2013.
- [44] A. Krizhevsky, I. Sutskever, and G. E. Hinton. Imagenet classification with deep convolutional neural networks. In *NIPS*, 2012.
- [45] M. La Cascia and E. Arduzzone. Jacob: Just a content-based query system for video databases. In *ICASSP*, 1996.
- [46] Y. LeCun, Y. Bengio, and G. Hinton. Deep learning. *Nature*, 521(7553):436–444, 2015.
- [47] J. Lee, J. Oh, and S. Hwang. Strg-index: Spatio-temporal region graph indexing for large video databases. In *SIGMOD*, 2005.
- [48] H. Li, Z. Lin, X. Shen, J. Brandt, and G. Hua. A convolutional neural network cascade for face detection. In *CVPR*, 2015.
- [49] T.-Y. Lin, M. Maire, S. Belongie, J. Hays, P. Perona, D. Ramanan, P. Dollár, and L. Zitnick. Microsoft coco: Common objects in context. In *ECCV*. European Conference on Computer Vision, September 2014.
- [50] D. G. Lowe. Object recognition from local scale-invariant features. In *ICCV*, 1999.
- [51] D. Lu and Q. Weng. A survey of image classification methods and techniques for improving classification performance. *International journal of Remote sensing*, 28(5):823–870, 2007.
- [52] H. Maamatou, T. Chateau, S. Gazzah, Y. Goyat, and N. E. Ben Amara. Sequential Monte Carlo filter based on multiple strategies for a scene specialization classifier. *EURASIP Journal on Image and Video Processing*, 2016(1):40, 2016.
- [53] C. Metz. AI is about to learn more like humans—with a little uncertainty. *Wired*, 2017. <https://www.wired.com/2017/02/ai-learn-like-humans-little-uncertainty/>.
- [54] A. Mhalla, H. Maamatou, T. Chateau, S. Gazzah, and N. E. B. Amara. Faster R-CNN scene specialization with a sequential Monte-Carlo framework. In *DICTA*, 2016.
- [55] K. Munagala, U. Srivastava, and J. Widom. Optimization of continuous queries with shared expensive filters. In *SIGMOD*, 2007.
- [56] D. Murray and A. Basu. Motion tracking with an active camera. *IEEE Trans. Pattern Anal. Mach. Intell.*, 16(5):449–459, May 1994.
- [57] V. E. Ogle and M. Stonebraker. Chabot: Retrieval from a relational database of images. *Computer*, 28(9):40–48, 1995.
- [58] J. Oh and K. A. Hua. Efficient and cost-effective techniques for browsing and indexing large video databases. In *SIGMOD*, 2000.
- [59] S. J. Pan and Q. Yang. A survey on transfer learning. *TKDE*, 22(10):1345–1359, 2010.
- [60] S. A. Papert. The summer vision project. 1966.
- [61] A. Patait and E. Young. High performance video encoding with NVIDIA GPUs. 2016 GPU Technology Conference (<http://on-demand.gputechconf.com/gtc/2016/presentation/s6226-abhijit-patait-high-performance-video.pdf>), 2016.
- [62] M. Rastegari, V. Ordonez, J. Redmon, and A. Farhadi. Xnor-net: Imagenet classification using binary convolutional neural networks. In *ECCV*, 2016.
- [63] B. Reagen, P. Whatmough, R. Adolf, S. Rama, H. Lee, S. K. Lee, J. M. Hernández-Lobato, G.-Y. Wei, and D. Brooks. Minerva: Enabling low-power, highly-accurate deep neural network accelerators. In *ISCA*, 2016.
- [64] J. Redmon, S. Divvala, R. Girshick, and A. Farhadi. You only look once: Unified, real-time object detection. *arXiv preprint arXiv:1506.02640*, 2015.
- [65] J. Redmon and A. Farhadi. Yolo9000: Better, faster, stronger. *arXiv preprint arXiv:1612.08242*, 2016.
- [66] S. Ren, K. He, R. Girshick, and J. Sun. Faster r-cnn: Towards real-time object detection with region proposal networks. In *NIPS*, 2015.
- [67] O. Russakovsky, J. Deng, H. Su, J. Krause, S. Satheesh, S. Ma, Z. Huang, A. Karpathy, A. Khosla, M. Bernstein, et al. Imagenet large scale visual recognition challenge. *International Journal of Computer Vision*, 115(3):211–252, 2015. <http://image-net.org/>.
- [68] P. G. Selinger, M. M. Astrahan, D. D. Chamberlin, R. A. Lorie, and T. G. Price. Access path selection in a relational database management system. In *SIGMOD*, 1979.
- [69] P. Sermanet, K. Kavukcuoglu, S. Chintala, and Y. LeCun. Pedestrian detection with unsupervised multi-stage feature learning. In *CVPR*, 2013.
- [70] Y. Sun, X. Wang, and X. Tang. Deep convolutional network cascade for facial point detection. In *CVPR*, 2013.
- [71] R. Szeliski. *Computer vision: algorithms and applications*. Springer Science & Business Media, 2010.
- [72] R. Verschae, J. Ruiz-del Solar, and M. Correa. A unified learning framework for object detection and classification using nested cascades of boosted classifiers. *Machine Vision and Applications*, 19(2):85–103, 2008.
- [73] P. Viola and M. Jones. Rapid object detection using a boosted cascade of simple features. In *CVPR*, 2001.
- [74] P. Weinzaepfel, Z. Harchaoui, and C. Schmid. Learning to track for spatio-temporal action localization. In *ICCV*, 2015.
- [75] A. Yoshitaka and T. Ichikawa. A survey on content-based retrieval for multimedia databases. *TKDE*, 11(1):81–93, 1999.

- [76] K.-H. Yu, C. Zhang, G. J. Berry, R. B. Altman, C. Ré, D. L. Rubin, and M. Snyder. Predicting non-small cell lung cancer prognosis by fully automated microscopic pathology image features. *Nature Communications*, 7, 2016.
- [77] C. Zhang et al. Extracting databases from dark data with deepdive. In *SIGMOD*, 2016.
- [78] S. Zhang, R. Benenson, M. Omran, J. Hosang, and B. Schiele. How far are we from solving pedestrian detection? In *CVPR*, 2016.
- [79] W. Zhao, R. Chellappa, P. J. Phillips, and A. Rosenfeld. Face recognition: A literature survey. *CSUR*, 35(4):399–458, 2003.
- [80] X. Zhu, X. Wu, A. K. Elmagarmid, Z. Feng, and L. Wu. Video data mining: Semantic indexing and event detection from the association perspective. *TKDE*, 17(5):665–677, 2005.